

Early differentiation and volatile accretion recorded in deep-mantle neon and xenon

Sujoy Mukhopadhyay¹

The isotopes ^{129}Xe , produced from the radioactive decay of extinct ^{129}I , and ^{136}Xe , produced from extinct ^{244}Pu and extant ^{238}U , have provided important constraints on early mantle outgassing and volatile loss from Earth^{1,2}. The low ratios of radiogenic to non-radiogenic xenon ($^{129}\text{Xe}/^{130}\text{Xe}$) in ocean island basalts (OIBs) compared with mid-ocean-ridge basalts (MORBs) have been used as evidence for the existence of a relatively undegassed primitive deep-mantle reservoir¹. However, the low $^{129}\text{Xe}/^{130}\text{Xe}$ ratios in OIBs have also been attributed to mixing between subducted atmospheric Xe and MORB Xe, which obviates the need for a less degassed deep-mantle reservoir^{3,4}. Here I present new noble gas (He, Ne, Ar, Xe) measurements from an Icelandic OIB that reveal differences in elemental abundances and $^{20}\text{Ne}/^{22}\text{Ne}$ ratios between the Iceland mantle plume and the MORB source. These observations show that the lower $^{129}\text{Xe}/^{130}\text{Xe}$ ratios in OIBs are due to a lower I/Xe ratio in the OIB mantle source and cannot be explained solely by mixing atmospheric Xe with MORB-type Xe. Because ^{129}I became extinct about 100 million years after the formation of the Solar System, OIB and MORB mantle sources must have differentiated by 4.45 billion years ago and subsequent mixing must have been limited. The Iceland plume source also has a higher proportion of Pu- to U-derived fission Xe, requiring the plume source to be less degassed than MORBs, a conclusion that is independent of noble gas concentrations and the partitioning behaviour of the noble gases with respect to their radiogenic parents. Overall, these results show that Earth's mantle accreted volatiles from at least two separate sources and that neither the Moon-forming impact nor 4.45 billion years of mantle convection has erased the signature of Earth's heterogeneous accretion and early differentiation.

The noble gases play an important role in understanding mantle structure and in quantifying mass and volatile fluxes into and out of the mantle^{1,5–10}. Interpretation of the differences in noble gas composition between MORBs and OIBs has primarily relied upon steady-state mantle models that require ^{129}Xe and primordial noble gases such as ^3He , ^{22}Ne and ^{36}Ar in the volatile-depleted upper mantle to be derived from a primitive volatile-rich lower mantle via plume mass flow^{8,9}. Mixtures of the plume-derived noble gases, radiogenic noble gases produced in the upper mantle, and subducted atmospheric Ar and Xe into the MORB source produce the noble gas isotopic compositions observed in MORBs. Such interpretations have been challenged on the grounds that a primitive lower mantle is at odds with geodynamic models of whole mantle convection¹¹, seismological observations of plate subduction into the lower mantle¹², and the depleted geochemical characteristics of OIBs¹³. However, the steady-state models could still be correct, if instead of the whole lower mantle, the primitive layer were much smaller, such as the D' layer at the base of the mantle⁹. Numerous alternative interpretations of the noble gas observations have also been proposed, particularly to explain high $^3\text{He}/^4\text{He}$ ratios in OIBs within the framework of whole mantle convection, as some geodynamic models suggest that preserving primitive layers over the age of the Earth is problematic¹¹. These interpretations assign high $^3\text{He}/^4\text{He}$ ratios to non-primordial processed mantle material^{14–16} and include the preservation of high $^3\text{He}/^4\text{He}$ ratios in U-Th depleted residues of mantle melting.

Relative elemental abundances of the noble gases and precise measurements of isotopic ratios of Ne, Ar and Xe can distinguish between the different hypotheses put forward to explain the noble gas observations. For example, the steady-state models predict that MORBs and OIBs should have the same elemental abundances and that MORB-Xe is related to OIB-Xe through addition of atmospheric and fission-produced Xe. Whereas the elemental abundance pattern and the isotopic ratios of the upper mantle are relatively well-defined^{3,17}, the composition of the OIB mantle source remains poorly known; this is because low noble gas concentrations and post-eruptive atmospheric contamination often result in the mantle Ne, Ar and Xe compositions being overprinted. To overcome this problem, single large pieces of the DICE 10 basaltic glass from Iceland^{18,19} were analysed by step-crushing under vacuum.

The new observations from Iceland show three steps where $^{20}\text{Ne}/^{22}\text{Ne}$ ratios reach 12.88 ± 0.06 , 12.76 ± 0.01 and 12.74 ± 0.02 (Fig. 1). These values are unequivocally higher than the upper-mantle composition of ≤ 12.5 , constrained from continental well gases^{3,20}. Previously, the only exceptions to a mantle $^{20}\text{Ne}/^{22}\text{Ne}$ ratio of ≤ 12.5 were carbonatites from the 380-Myr-old plume in the Kola peninsula of Russia, with a maximum measured $^{20}\text{Ne}/^{22}\text{Ne}$ of 13.04 ± 0.2 (ref. 21). Thus, the Kola and Iceland plumes require the $^{20}\text{Ne}/^{22}\text{Ne}$ ratio of the MORB and plume sources to be different. Because ^{20}Ne and ^{22}Ne are primordial, and atmospheric Ne is not subducted back into the mantle in significant quantities³, the $^{20}\text{Ne}/^{22}\text{Ne}$ ratio in the mantle does not evolve over time. Consequently, the new observations from Iceland and those from the Kola plume suggest that at least two separate reservoirs contributed neon during Earth's accretion²⁰.

Elemental abundance ratios provide additional insights into the origin of the observed difference in $^{20}\text{Ne}/^{22}\text{Ne}$ composition between MORBs and OIBs. The noble gases have different solubilities in a basalt melt, and so magmatic degassing will fractionate the elemental ratios in the melt compared to the mantle source. The relative abundances of ^4He , ^{21}Ne and ^{40}Ar in the DICE 10 sample are, however, in the same proportion as the mantle production rates for these isotopes (Supplementary Fig. 3), indicating that the sample preserves unfractionated mantle elemental ratios.

Excellent correlations are observed between isotope ratios and elemental ratios, allowing precise determination of the mantle source elemental abundance ratios. Figure 2 demonstrates that the Iceland plume has a lower $^3\text{He}/^{22}\text{Ne}$ ratio than the MORB source, consistent with previous observations that plume and MORB sources may have different $^3\text{He}/^{22}\text{Ne}$ ratios^{18,22}. In addition, the new Icelandic observations indicate that the plume source has higher $^3\text{He}/^{36}\text{Ar}$ and $^{22}\text{Ne}/^{36}\text{Ar}$ ratios than the MORB source (Fig. 2; Supplementary Table 1). Although the high-pressure behaviours of the noble gases are not well constrained, the differences in the elemental abundance ratios between MORBs and the Iceland sample do not appear to be linked in any systematic way to diffusive fractionation or ancient magmatic degassing, such as degassing from a magma ocean (Fig. 2). Thus, the differences in $^{20}\text{Ne}/^{22}\text{Ne}$ and $^3\text{He}/^{22}\text{Ne}$ ratios observed between the Iceland source and the MORB source probably reflect an accretional

¹Department of Earth and Planetary Sciences, Harvard University, Cambridge, Massachusetts 02138, USA.

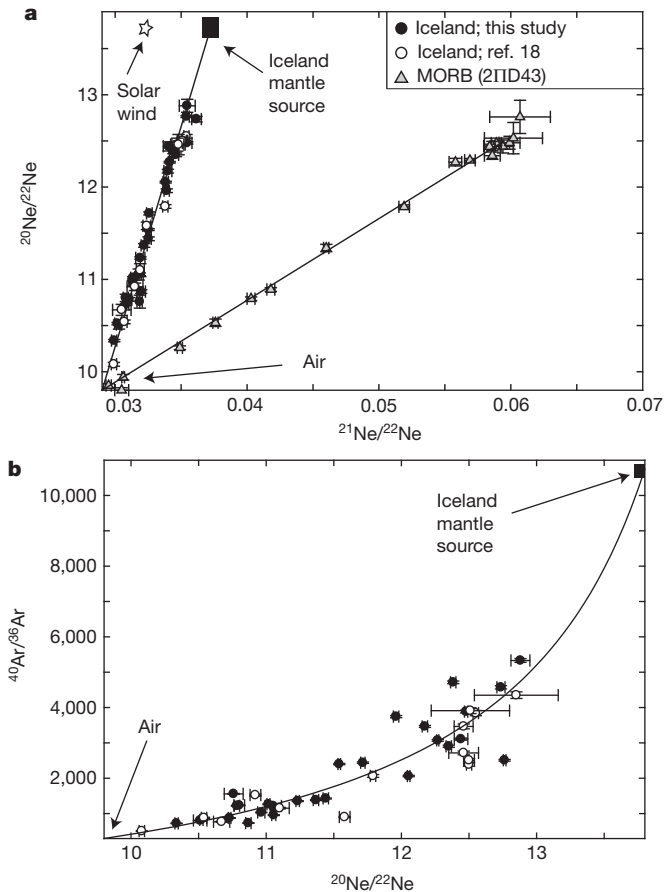


Figure 1 | Differences in neon and argon isotopic composition between MORB and the Iceland plume. **a**, Neon three-isotope plot showing the new analyses of the DICE 10 sample (filled circles) from Iceland in comparison to previously published data for this sample (open circles; ref. 18) and the gas-rich ‘popping rock’ (2IID43) from the north Mid-Atlantic Ridge (open triangles; ref. 17). Error bars are 1σ , and for clarity, two previous analyses¹⁸ with large error bars have not been shown. Step-crushing of a mantle-derived basalt produces a linear trend that reflects variable amounts of post-eruptive air contamination in vesicles containing mantle Ne. The slope of the line is a function of the ratio of nucleogenic ^{21}Ne to primordial ^{22}Ne , with steeper slopes indicating a higher proportion of primordial ^{22}Ne and, thus, a less degassed mantle source. The slope of the Iceland line based on the new analyses is consistent with that obtained previously¹⁸. Importantly, $^{20}\text{Ne}/^{22}\text{Ne}$ ratios of 12.88 ± 0.06 are distinctly higher than the MORB source $^{20}\text{Ne}/^{22}\text{Ne}$ of ≤ 12.5 as constrained from continental well gases²⁰. **b**, Ne–Ar compositions of individual step crushes of the DICE 10 sample. ^{40}Ar is generated by radioactive decay of ^{40}K , and low $^{40}\text{Ar}/^{36}\text{Ar}$ ratios are indicative of a less degassed mantle. The data reflect mixing between a mantle component and post-eruptive atmospheric contamination. A least-squares hyperbolic fit through the data yields a $^{40}\text{Ar}/^{36}\text{Ar}$ ratio of $10,745 \pm 3,080$, corresponding to a mantle solar $^{20}\text{Ne}/^{22}\text{Ne}$ ratio of 13.8. This Ar isotopic ratio is used as the mantle source value for Iceland in Figs 2 and 3. Symbols as in **a**; error bars are 1σ .

signal, with the MORB mantle more similar to the meteoritic Ne-B²⁰ composition and the deep mantle similar to a solar Ne composition^{20,21}.

Taken together, the differences in $^{20}\text{Ne}/^{22}\text{Ne}$, He/Ne and Ne/Ar ratios between MORBs and the Iceland plume require that heterogeneities from the early Earth still exist in the present day mantle, and the new Xe measurements provide conclusive evidence for this interpretation. Previous studies have observed lower $^{129}\text{Xe}/^{130}\text{Xe}$ ratios in OIBs compared to MORBs^{3,17,18}. The lower measured $^{129}\text{Xe}/^{130}\text{Xe}$ ratios in OIBs could reflect syn- to post-eruptive atmospheric contamination of the lavas, mixing between subducted atmospheric Xe and MORB-type Xe^{3,4,18}, or different I/Xe ratios for the plume and MORB sources¹. Ar–Xe mixing systematics (Fig. 3) constrain the Iceland mantle source $^{129}\text{Xe}/^{130}\text{Xe}$ ratio to be 6.98 ± 0.07 , significantly lower than the MORB source ratio of 7.9 ± 0.14 (ref. 3). Therefore, syn- to post-eruptive

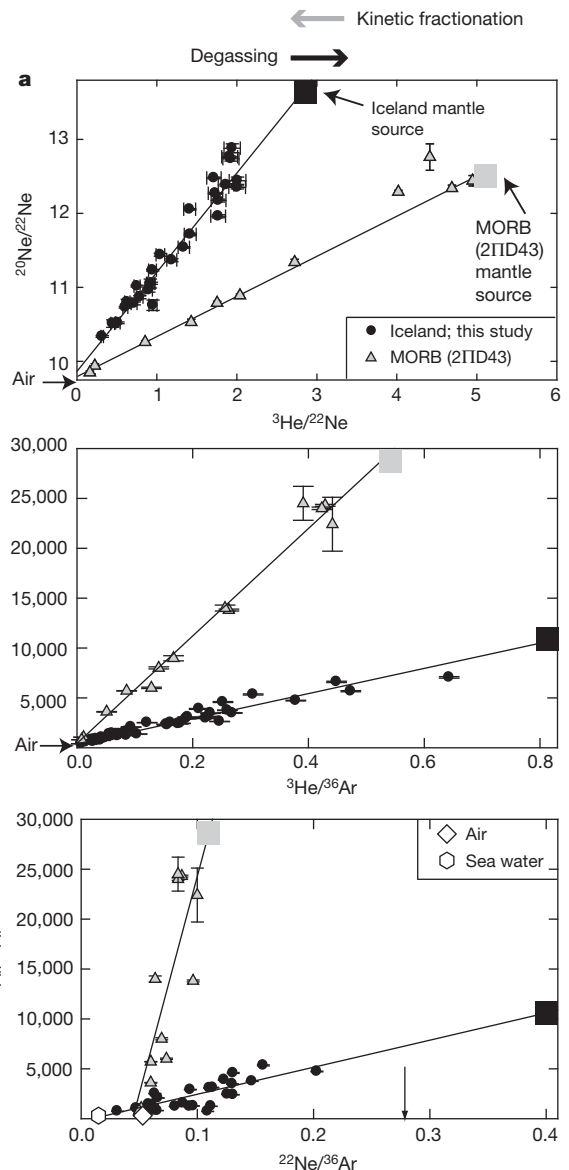


Figure 2 | Differences in elemental abundances and isotope ratios between MORB and the Iceland plume. Error bars are 1σ . **a**, $^3\text{He}/^{22}\text{Ne}$ versus $^{20}\text{Ne}/^{22}\text{Ne}$; **b**, $^3\text{He}/^{36}\text{Ar}$ versus $^{40}\text{Ar}/^{36}\text{Ar}$; and **c**, $^{22}\text{Ne}/^{36}\text{Ar}$ versus $^{40}\text{Ar}/^{36}\text{Ar}$. The mantle source composition for 2IID43 (filled grey square in all panels) is based on the $^{40}\text{Ar}/^{36}\text{Ar}$ and $^{20}\text{Ne}/^{22}\text{Ne}$ ratios as defined in ref. 30, and the mantle source composition for Iceland (filled black square in all panels) is based on Fig. 1. The grey and black arrows at the top of the figure indicate how elemental ratios evolve as a result of kinetic fractionation and solubility controlled degassing, respectively. Good linear relationships are observed between isotope ratios and elemental ratios, which reflect mixing between mantle-derived noble gases and post-eruptive atmospheric contamination. Lines are robust linear regressions through the data with the atmospheric contaminant near the origin and the mantle source at the other end. Arrow in **c** indicates the minimum $^{22}\text{Ne}/^{36}\text{Ar}$ ratio of the Iceland mantle source given the measured $^{40}\text{Ar}/^{36}\text{Ar}$ ratio of 7,047 (Supplementary Table 6). Because of systematic differences in noble gas solubilities and diffusivities, the differences in elemental abundances are not likely to be generated through ancient fractionation associated with diffusion or magmatic outgassing. For example, kinetic fractionation should lead to higher $^3\text{He}/^{22}\text{Ne}$ and higher $^3\text{He}/^{36}\text{Ar}$ – $^{22}\text{Ne}/^{36}\text{Ar}$ ratios. However, the Iceland source has a lower $^3\text{He}/^{22}\text{Ne}$ and higher $^3\text{He}/^{36}\text{Ar}$ – $^{22}\text{Ne}/^{36}\text{Ar}$. Likewise, adding recycled atmospheric gases to the MORB source cannot produce the plume noble gas compositions. Finally, **c** shows that preferential recirculation of atmospheric Ar into the plume source does not explain the higher $^{22}\text{Ne}/^{36}\text{Ar}$ of the plume source and because of the difference in MORB and OIB $^{22}\text{Ne}/^{36}\text{Ar}$ ratios, adding radiogenic ^{40}Ar to the plume composition is not likely to generate the $^{40}\text{Ar}/^{36}\text{Ar}$ ratio in MORBs.

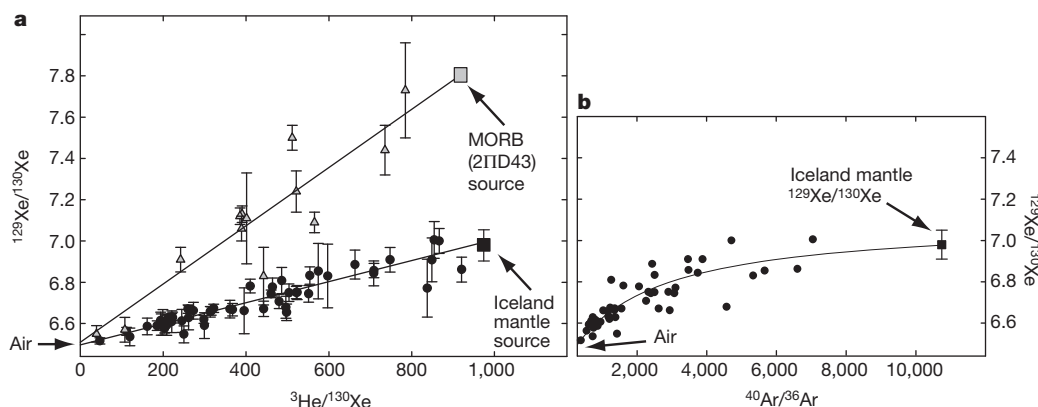


Figure 3 | Differences in Xe isotopic composition between MORB and the Iceland plume. **a**, Correlation between ^{129}Xe and ^3He in the ‘popping rock’ MORB (2IID43)¹⁷ and Iceland (DICE 10). Error bars are 1σ . Data points are individual step crushes that reflect different degrees of post-eruptive atmospheric contamination in the vesicles. Air lies near the origin and the mantle compositions at the other end of the linear arrays. The straight lines are robust regressions through the data. Because mixing in this space is linear, the lines also represent the trajectories along which the mantle sources will evolve when mixed

contamination processes are ruled out as the reason for the lower $^{129}\text{Xe}/^{130}\text{Xe}$ ratios at Iceland.

The data in Fig. 3a demonstrate that the Iceland and MORB source mantles evolved with different I/Xe ratios, requiring the two mantle sources to have separated by 4.45 Gyr ago with limited subsequent mixing between the two. As atmosphere is located near the origin in this plot (Fig. 3a), and mixing in this space is linear, adding subducted atmospheric Xe to the MORB source clearly cannot produce the Iceland mantle source composition. Similarly, the Iceland source cannot supply Xe to the MORB source unless it is augmented by radiogenic ^{129}Xe produced from decay of ^{129}I . However, ^{129}I became extinct at ~ 4.45 Gyr ago. Therefore, the two sources must have been separated before 4.45 Gyr ago and subsequently the sources were not homogenized, as otherwise the differences in $^{129}\text{Xe}/^{130}\text{Xe}$ would not have been preserved in the present day mantle. Plumes, therefore, cannot have supplied Xe and all of the primordial volatiles to the MORB source (Figs 1–3), contradicting predictions of the steady-state mantle models^{8,9}.

The new Xe isotopic measurements also indicate a difference in $^{129}\text{Xe}/^{136}\text{Xe}$ ratios between MORBs and the Iceland plume that cannot be related solely to subduction of atmospheric Xe, or to addition of ^{136}Xe to MORB Xe (Fig. 4). ^{136}Xe , along with ^{131}Xe , ^{132}Xe and ^{134}Xe , is produced by fission from extinct ^{244}Pu (half-life 80 Myr) and extant ^{238}U . However, Pu and U produce the four fission Xe isotopes in different proportions, and so measurements of the fissionogenic isotopes can be used to deconvolve Pu- from U-derived Xe (ref. 23). A reservoir that has remained closed to volatile loss over Earth history should have $\sim 97\%$ of the fission Xe isotopes produced from ^{244}Pu . Progressive degassing of a reservoir, particularly after ^{244}Pu becomes extinct, leads to increasing proportions of U-derived fission Xe in the reservoir.

Compared to the MORB source, the Iceland plume source has a substantially higher proportion of Pu- to U-derived fission Xe. Thus, the Iceland plume source is less degassed than the MORB source. Depending on whether the initial Xe isotopic composition of the mantle was solar or chondritic²⁴, the MORB source has a few per cent to $43 \pm 16\%$ of fission ^{136}Xe derived from ^{244}Pu . The corresponding values for Iceland are $66 \pm 19\%$ to $99^{+1}_{-3}\%$ (Supplementary Table 4); the latter value, based on an initial chondritic mantle Xe composition, is identical to values expected for closed system evolution. Hence, irrespective of the initial Xe isotopic composition of the mantle, the Iceland plume sample has a higher proportion of Pu- to U-derived fission Xe compared to MORB samples when both sets of data are processed in the same manner during the deconvolution (Methods, Supplementary Table 4). The requirement for a lower degree of degassing for the Iceland

with subducted air. The new observations from Iceland demonstrate that the Iceland plume $^{129}\text{Xe}/^{130}\text{Xe}$ ratio cannot be generated solely through adding recycled atmospheric Xe to the MORB source, and vice versa. Thus, two mantle reservoirs with distinct I/Xe ratios are required. The mantle $^{129}\text{Xe}/^{130}\text{Xe}$ ratio of 6.98 ± 0.07 for Iceland was derived from a hyperbolic least-squares fit through the Ar–Xe data (b) corresponding to a mantle $^{40}\text{Ar}/^{36}\text{Ar}$ ratio of 10,745. Note that given the curvature in Ar–Xe space, the $^{129}\text{Xe}/^{130}\text{Xe}$ in the Iceland mantle source is not particularly sensitive to the exact choice of the mantle $^{40}\text{Ar}/^{36}\text{Ar}$ ratio.

source, based on its higher proportion of Pu- to U-derived fission Xe, is a conclusion that is independent of the absolute concentrations of noble gases and the relative partition coefficients of the noble gases with respect to their radiogenic parents.

The combined I–Pu–Xe system has been used to constrain the closure time for volatile loss of a mantle reservoir through the $^{129}\text{Xe}/^{136}\text{Xe}_{\text{Pu}}$ ratio^{1,2,6,25}, where ^{129}Xe is the decay product of ^{129}I decay and $^{136}\text{Xe}_{\text{Pu}}$ is ^{136}Xe produced from ^{244}Pu fission. ^{129}I has a shorter half-life than ^{244}Pu , and as a result higher $^{129}\text{Xe}/^{136}\text{Xe}_{\text{Pu}}$ ratios are indicative of earlier closure to volatile loss^{1,2,6,25}. Depending on the initial mantle Xe composition, the $^{129}\text{Xe}/^{136}\text{Xe}_{\text{Pu}}$ ratio varies between $2.9^{+0.1}_{-0.1}$ and $5.8^{+1.1}_{-0.9}$ for the Iceland mantle and the corresponding values for MORBs are between $7.9^{+3.3}_{-2.9}$ and $64.9^{+132}_{-31.2}$ (Methods; Supplementary Table 4). If the mantle had a homogenous I/Pu ratio, the lower $^{129}\text{Xe}/^{136}\text{Xe}_{\text{Pu}}$ ratio in the plume source would paradoxically imply that the deep mantle became closed to volatile loss after the shallow mantle. A simpler explanation is that the lower $^{129}\text{Xe}/^{136}\text{Xe}_{\text{Pu}}$ ratio reflects a lower I/Pu ratio for the plume source compared to the MORB source. These differences would indicate that the initial phase of Earth’s accretion was volatile-poor compared to the later stages of accretion, a conclusion consistent with a recent Pd–Ag study²⁶.

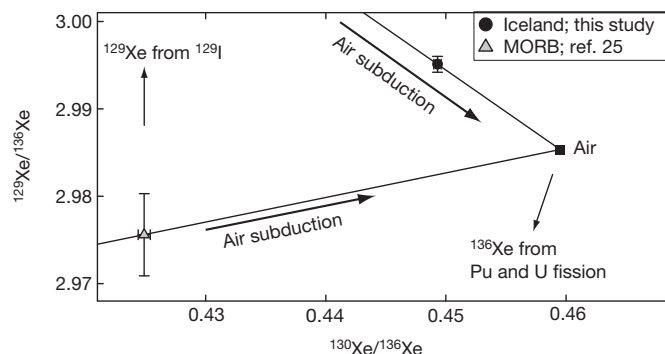


Figure 4 | Difference in the measured $^{129}\text{Xe}/^{136}\text{Xe}$ ratio between MORB and the Iceland plume. Unlike the traditional $^{129}\text{Xe}/^{130}\text{Xe}$ – $^{136}\text{Xe}/^{130}\text{Xe}$ plot, the x and y errors are de-correlated. The arrows illustrate how the MORB and OIB source compositions evolve as subducted air is added. Error bars are 1σ . The figure demonstrates a small Xe isotopic difference between the Iceland plume and MORBs that cannot be related solely through recycling atmospheric Xe or by adding fissionogenic ^{136}Xe to MORB Xe. The data points represent the weighted means of the different step crushes for MORBs ($n = 38$) and Iceland ($n = 51$; this study). The MORB $^{129}\text{Xe}/^{136}\text{Xe}$ ratio was calculated from the weighted means of the $^{129}\text{Xe}/^{130}\text{Xe}$ and $^{136}\text{Xe}/^{130}\text{Xe}$ ratios²⁵.

The long-term separation of the plume and MORB sources inferred from the $^{129}\text{Xe}/^{130}\text{Xe}$ ratio (Fig. 3), and the lower degree of outgassing of the plume source inferred from fission Xe, have implications for interpreting the differences in $^3\text{He}/^4\text{He}$ ratios between plumes and MORBs. It suggests that the high $^3\text{He}/^4\text{He}$ ratios observed in many mantle plumes are from an ancient reservoir created within the first 100 Myr of Solar System history, and that the high $^3\text{He}/^4\text{He}$ ratios reflect a lower degree of outgassing of the plume source compared to the MORB source. However, the incorporation of noble gases into the deep mantle appears to be associated with lower abundances (compared to the MORB source) of other volatiles, such as iodine and water. Subsequent processing, through partial melting of the mantle, led to a greater degree of volatile loss from the MORB source, with differences in the MORB and plume mantle sources established by 4.45 Gyr ago.

I note that the persistence of two different mantle Xe reservoirs established by 4.45 Gyr ago may seem to conflict with the homogeneous $^{142}\text{Nd}/^{144}\text{Nd}$ in the present-day mantle and crust²⁷. A possible explanation is the low recycling efficiency of the noble gases into the mantle compared to the lithophile elements. For example, compared to the present mantle, the Hadean mantle had a 20 p.p.m. excess in $^{142}\text{Nd}/^{144}\text{Nd}$ that was subsequently erased through crustal recycling and mixing²⁷. In addition, the observed heterogeneity in Xe isotopic composition compared to $^{142}\text{Nd}/^{144}\text{Nd}$ could be related to the magnitude of I–Xe and Pu–Xe fractionations during partial melting and magmatic degassing, which led to larger Xe isotopic anomalies compared to $^{142}\text{Nd}/^{144}\text{Nd}$. In any case, since the chemical differences established very early in Earth's history are still preserved in the $^{129}\text{Xe}/^{130}\text{Xe}$ ratios, direct mixing between the MORB and plume reservoirs since 4.45 Gyr ago must have been limited.

The preservation of an ancient mantle reservoir has important implications for Earth evolution. For example, although it has been hypothesized that the Moon-forming giant impact led to homogenization of the mantle²⁸, the Ne and Xe isotopic heterogeneities suggest that complete homogenization did not occur. Finally, whether the primordial noble gases that supply mantle plumes are distributed throughout the whole lower mantle or are localized in a region of the deep mantle—such as the large low-shear-wave-velocity provinces (LLSVPs) at the base of the mantle²⁹—can be debated. However, if noble gases in plumes are derived from the LLSVPs²⁹, then based on the new Xe evidence, LLSVPs are features that have existed since the formation of the Earth and cannot exclusively be composed of subducted slabs.

METHODS SUMMARY

To minimize contamination by air adsorbed on the sample surface, single large pieces of the DICE 10 glass (~2.2–3.5 g) from Iceland were analysed. Gases were released by step-crushing under vacuum and noble gas abundances and isotopic ratios were determined using a Nu Noblesse multi-collector mass spectrometer (Supplementary Tables 5–7). Mass discrimination was monitored through sample-standard bracketing using air as a standard.

Deconvolution of U- from Pu-derived fission Xe was done using five Xe isotopes (^{130}Xe , ^{131}Xe , ^{132}Xe , ^{134}Xe , ^{136}Xe). To investigate whether the conclusion of a higher Pu- to U-derived fission Xe for Iceland is robust, three different initial mantle Xe isotopic compositions were investigated: U-Xe, solar wind Xe and chondritic Xe. Furthermore, two different techniques were used to compute the mantle source fission isotopic compositions. In the first technique, the atmospheric Xe isotopic ratios were linearly projected to a mantle source value of $^{129}\text{Xe}/^{132}\text{Xe}$ through the weighted averages of the measured Xe isotopic ratios (Methods). In the second technique, $^{136}\text{Xe}/^{130}\text{Xe}$ ratios in the individual steps were regressed against $^{129}\text{Xe}/^{130}\text{Xe}$ ratios. Given the mantle $^{129}\text{Xe}/^{130}\text{Xe}$ ratio (Fig. 3), the mantle $^{136}\text{Xe}/^{130}\text{Xe}$ was computed from the best-fit slopes. The mantle values for the other fission isotope ratios were then established by regressing the Xe isotopic ratios in individual steps against the $^{136}\text{Xe}/^{130}\text{Xe}$ ratio. The fission isotopic compositions were used to solve the system of equations $Ax = b$ with $\sum x_i = 1$ and $0 \leq x_i \leq 1$, where A defines the end-member compositions (recycled air, initial mantle Xe, Pu- and U-derived Xe), x the fraction of each end-member, and b the mantle source composition. To compute the uncertainties, a Monte Carlo technique was used whereby the estimated sample compositions were varied at random within the 1 σ uncertainty and the least squares fit recomputed.

Full Methods and any associated references are available in the online version of the paper at www.nature.com/nature.

Received 7 November 2011; accepted 11 April 2012.

- Allège, C. J., Staudacher, T. & Sarda, P. Rare gas systematics: formation of the atmosphere, evolution and structure of the Earth's mantle. *Earth Planet. Sci. Lett.* **81**, 127–150 (1987).
- Marty, B. Neon and xenon isotopes in MORB: implications for the earth-atmosphere evolution. *Earth Planet. Sci. Lett.* **94**, 45–56 (1989).
- Holland, G. & Ballentine, C. J. Seawater subduction controls the heavy noble gas composition of the mantle. *Nature* **441**, 186–191 (2006).
- Trieloff, M. & Kunz, J. Isotope systematics of noble gases in the Earth's mantle: possible sources of primordial isotopes and implications for mantle structure. *Phys. Earth Planet. Inter.* **148**, 13–38 (2005).
- Gonnermann, H. M. & Mukhopadhyay, S. Preserving noble gases in a convecting mantle. *Nature* **459**, 560–563 (2009).
- Yokochi, R. & Marty, B. Geochemical constraints on mantle dynamics in the Hadean. *Earth Planet. Sci. Lett.* **238**, 17–30 (2005).
- Pepin, R. O. & Porcelli, D. Origin of noble gases in the terrestrial planets. *Rev. Mineral. Geochem.* **47**, 191–246 (2002).
- Porcelli, D. & Wasserburg, G. J. Mass transfer of helium, neon, argon and xenon through a steady-state upper mantle. *Geochim. Cosmochim. Acta* **59**, 4921–4937 (1995).
- Tolstikhin, I. & Hofmann, A. W. Early crust on top of the Earth's core. *Phys. Earth Planet. Inter.* **148**, 109–130 (2005).
- Kurz, M. D., Jenkins, W. J. & Hart, S. R. Helium isotopic systematics of oceanic islands and mantle heterogeneity. *Nature* **297**, 43–47 (1982).
- Brandenburg, J. P., Hauri, E. H., van Keken, P. E. & Ballentine, C. J. A multiple-system study of the geochemical evolution of the mantle with force-balanced plates and thermochemical effects. *Earth Planet. Sci. Lett.* **276**, 1–13 (2008).
- van der Hilst, R. D. & Karason, H. Compositional heterogeneity in the bottom 1000 kilometers of Earth's mantle: toward a hybrid convection model. *Science* **283**, 1885–1888 (1999).
- Class, C. & Goldstein, S. L. Evolution of helium isotopes in the Earth's mantle. *Nature* **436**, 1107–1112 (2005).
- Albarede, F. Rogue mantle helium and neon. *Science* **319**, 943–945 (2008).
- Parmar, S. W. Helium isotopic evidence for episodic mantle melting and crustal growth. *Nature* **446**, 900–903 (2007).
- Lee, C. T. A. *et al.* Upside-down differentiation and generation of a 'primordial' lower mantle. *Nature* **463**, 930–933 (2010).
- Moreira, M., Kunz, J. & Allegre, C. Rare gas systematics in popping rock: isotopic and elemental compositions in the upper mantle. *Science* **279**, 1178–1181 (1998).
- Trieloff, M., Kunz, J., Clague, D. A., Harrison, D. & Allegre, C. J. The nature of pristine noble gases in mantle plumes. *Science* **288**, 1036–1038 (2000).
- Harrison, D., Burnard, P. G., Trieloff, M. & Turner, G. Resolving atmospheric contaminants in mantle noble gas analyses. *Geochem. Geophys. Geosyst.* **4**, 1023 (2003).
- Ballentine, C. J., Marty, B., Lollar, B. S. & Cassidy, M. Neon isotopes constrain convection and volatile origin in the Earth's mantle. *Nature* **433**, 33–38 (2005).
- Yokochi, R. & Marty, B. A determination of the neon isotopic composition of the deep mantle. *Earth Planet. Sci. Lett.* **225**, 77–88 (2004).
- Honda, M. & McDougall, I. Primordial helium and neon in the Earth — a speculation on early degassing. *Geophys. Res. Lett.* **25**, 1951–1954 (1998).
- Caffee, M. W. *et al.* Primordial noble gases from Earth's mantle: identification of a primitive volatile component. *Science* **285**, 2115–2118 (1999).
- Pujol, M., Marty, B. & Burgess, R. Chondritic-like xenon trapped in Archean rocks: a possible signature of the ancient atmosphere. *Earth Planet. Sci. Lett.* **308**, 298–306 (2011).
- Kunz, J., Staudacher, T. & Allegre, C. J. Plutonium-fission xenon found in Earth's mantle. *Science* **280**, 877–880 (1998).
- Schonbachler, M., Carlson, R. W., Horan, M. F., Mock, T. D. & Hauri, E. H. Heterogeneous accretion and the moderately volatile element budget of Earth. *Science* **328**, 884–887 (2010).
- Caro, G. Early silicate Earth differentiation. *Annu. Rev. Earth Planet. Sci.* **39**, 31–58 (2011).
- Pahlevan, K. & Stevenson, D. J. Equilibration in the aftermath of the lunar-forming giant impact. *Earth Planet. Sci. Lett.* **262**, 438–449 (2007).
- Torsvik, T. H., Burke, K., Steinberger, B., Webb, S. J. & Ashwal, L. D. Diamonds sampled by plumes from the core–mantle boundary. *Nature* **466**, 352–355 (2010).
- Raquin, A., Moreira, M. A. & Guillou, F. He, Ne and Ar systematics in single vesicles: mantle isotopic ratios and origin of the air component in basaltic glasses. *Earth Planet. Sci. Lett.* **274**, 142–150 (2008).

Supplementary Information is linked to the online version of the paper at www.nature.com/nature.

Acknowledgements I thank D. Graham for supplying the Iceland sample, and K. Zahnle, C. Langmuir, S. Stewart and R. Parai for comments. Reviews by C. Ballentine, B. Marty and D. Porcelli helped to improve the paper. This work was supported by NSF grant EAR 0911363.

Author Information Reprints and permissions information is available at www.nature.com/reprints. The author declares no competing financial interests. Readers are welcome to comment on the online version of this article at www.nature.com/nature. Correspondence and requests for materials should be addressed to the author (sujoy@eps.harvard.edu).

METHODS

Mass spectrometry. Five separate analyses were performed on single large pieces (~2.2–3.5 g) of the DICE 10 basaltic glass from the Reykjanes Peninsula in Iceland¹⁸ by step-crushing. The glass piece was loaded into the vacuum crusher, baked at ~90–100 °C for 18 h and then pumped for an additional 10–14 days until blanks were stable and low. To release magmatic volatiles, the glass was crushed in a step-wise manner with a hydraulic ram. The released gases were purified by sequential exposure to hot and cold SAES getters and a small split of the gas was let into a quadrupole mass spectrometer to determine the Ar abundance and an approximate $^{40}\text{Ar}/^{36}\text{Ar}$ ratio. The noble gases were then trapped on a cryogenic cold-finger. He was separated from Ne at 32 K and let into the Nu Noblesse mass spectrometer. The measurements were carried out at 200 μA trap current and an electron accelerating voltage of 60 eV.

After the He measurement was completed, the cryogenic trap was warmed to 74 K to separate Ne from Ar. Ne was measured in multi-collection mode using three discrete dynode multipliers. ^{21}Ne was measured on the axial multiplier fitted with an energy filter, while ^{20}Ne and ^{22}Ne were measured on the low and high mass multipliers, respectively. For ^{20}Ne beams larger than 100,000 counts per second ($\sim 3.9 \times 10^{-10} \text{ cm}^3$ of ^{20}Ne), ^{20}Ne was measured on a Faraday cup while ^{21}Ne and ^{22}Ne were measured on the low mass multiplier in single collection mode. An automated liquid nitrogen trap was used to keep the Ar and CO_2 backgrounds low and isobaric interferences from doubly-charged Ar and CO_2 were corrected for. The $\text{Ar}^{2+}/\text{Ar}^+$ ratios for the three sets of Ne measurements were 0.03 ± 0.002 , 0.034 ± 0.003 and 0.031 ± 0.003 , while the corresponding $\text{CO}_2^{2+}/\text{CO}_2^+$ ratios were 0.0039 ± 0.001 , 0.0035 ± 0.0008 and 0.0045 ± 0.0005 , respectively. No significant variations were observed in these ratios as a function of Ar, CO_2 or H_2 partial pressure in the mass spectrometer, and the Ar^{2+} and CO_2^{2+} corrections for all step crushes were $<1\%$.

Following the Ne measurement, the cold-finger was warmed to 185 K to release Ar, and depending upon the Ar abundance and approximate isotope ratio previously determined by the quadrupole mass spectrometer, a fraction of the gas was let into the mass spectrometer for more precise isotope ratio determination. The Ar isotopes were measured in multi-collection mode with ^{40}Ar on the Faraday cup, and ^{38}Ar and ^{36}Ar were measured on the axial and low mass multipliers, respectively.

Kr was not measured and to separate Kr from Xe, the cold-finger was warmed to 210 K to release Kr which was pumped away. The cold-finger was then warmed to 340 K to release all of the Xe. Xenon isotopes were measured in a combination of multi-collection and peak-jumping mode in the following five steps: $^{126-132}\text{Xe}$, $^{128-134}\text{Xe}$, $^{124-130-136}\text{Xe}$, ^{129}Xe , ^{131}Xe , ^{124}Xe and ^{126}Xe are the two rarest Xe isotopes, and since sufficient time was not spent counting these isotopes, they are not reported here.

The total procedural blanks for ^4He , ^{22}Ne , ^{36}Ar and ^{130}Xe before starting the crush were (in cm^3) $\leq 2 \times 10^{-11}$, $\leq 3 \times 10^{-14}$, $\leq 4 \times 10^{-13}$ and $\leq 1.5 \times 10^{-16}$, respectively. Blanks were monitored during the course of the step-crushes. With the exception of the He blank, which increased by up to a factor of 2–4, Ne, Ar and Xe blanks were either stable or decreased with progressive sample crushing. Ne, Ar and Xe blank isotopic ratios were statistically indistinguishable from atmosphere, and because the sample gases are a mixture of mantle and air, no blank corrections were applied to any of the step crushes. Mass discrimination for Ne, Ar and Xe isotope ratios was determined with air standards and instrumental drift was monitored through sample-standard bracketing with additional standards run overnight.

Hyperbolic fits. Least-squares hyperbolic fits were computed using the curve fitting tool in Matlab. Since the fits were constrained to go through atmospheric composition, the data were fitted with an equation of the form $ax + bxy + cy = 0$. **Deconvolving U- from Pu-derived fissionogenic Xe.** Before discussing the deconvolution of Pu- to U-derived fission Xe, I note that Iceland and the MORB source have different fission isotopic compositions that cannot be related to each other solely through addition of atmospheric Xe. In ^{130}Xe -normalized fission isotope spaces (such as $^{136}\text{Xe}/^{130}\text{Xe}$ versus $^{132}\text{Xe}/^{130}\text{Xe}$), the Iceland sample always defines a steeper slope than MORBs when the regressions are done using individual steps (Supplementary Table 2) or using the weighted mean composition of the sample (Supplementary Fig. 5). Thus, irrespective of the exact proportions of the Pu- to U-derived fission Xe, Supplementary Table 3 and Supplementary Fig. 5 demonstrate a difference in Pu- to U-derived fission Xe between MORBs and the Iceland plume.

To deconvolve U- from Pu-derived fissionogenic Xe, five Xe isotopes were used ($^{130,131,132,134,136}\text{Xe}$). In mantle-derived basalts, vesicles have different degrees of post-eruptive atmospheric Xe contamination. To demonstrate that differences between Iceland and MORB fission Xe isotopes are robust, two different methods were used to determine the mantle fission Xe isotopic ratios free of post-eruptive air contamination.

First, the weighted means of the fissionogenic isotope ratios ($^{130}\text{Xe}/^{132}\text{Xe}$, $^{131}\text{Xe}/^{132}\text{Xe}$, $^{134}\text{Xe}/^{132}\text{Xe}$, $^{136}\text{Xe}/^{132}\text{Xe}$) were calculated from the 51 Icelandic measurements (Supplementary Table 7). The atmospheric $^{130,131,134,136}\text{Xe}/^{132}\text{Xe}$ ratios were then linearly projected to a mantle $^{129}\text{Xe}/^{132}\text{Xe}$ ratio of 1.032 (Supplementary Fig. 4) through the weighted average of the Iceland measurements. For MORBs, fission isotopes are reported normalized to ^{130}Xe ($^{131,132,134,136}\text{Xe}/^{130}\text{Xe}$)⁴. Hence, the weighted mean of the ^{130}Xe normalized ratios were computed. The atmospheric $^{131,132,134,136}\text{Xe}/^{130}\text{Xe}$ ratios were then linearly projected to a mantle $^{129}\text{Xe}/^{130}\text{Xe}$ ratio of 7.8 (refs 3, 17) through the weighted average of the MORB measurements, and the ^{132}Xe -normalized mantle source fission ratios were subsequently computed. These compositions represent Iceland-1 and MORB-1 in Supplementary Tables 3 and 4. Note that to process both data sets the same way, the weighted means for Iceland and MORBs were calculated without eliminating any data points.

Second, for Iceland and MORBs, the $^{136}\text{Xe}/^{130}\text{Xe}$ ratios in the individual steps were regressed against the $^{129}\text{Xe}/^{130}\text{Xe}$ ratios. Because one is interested in the slope of the best fit lines, data points were translated such that the atmospheric composition was at (0,0). The y data were then scaled by the square root of the ratio of the variance in x to the variance in y so as to put x and y on the same scale and fitted with an equation of the form $y = mx$. The x and y error-weighted best fit slope was computed by minimizing the value of χ^2 . The uncertainty in the slope was calculated with a Monte Carlo method; the x and y data were varied at random, the best-fit line recomputed and the 67% confidence limit on the best fit line determined subsequently. The best fit line and the uncertainty in the slope were then scaled back to the original coordinate system.

From the slope and uncertainty in the slope, the mantle $^{136}\text{Xe}/^{130}\text{Xe}$ ratio, along with its uncertainty, were calculated for mantle $^{129}\text{Xe}/^{130}\text{Xe}$ ratios of 6.98 and 7.8 for Iceland and MORB sources, respectively (Fig. 3). $^{131}\text{Xe}/^{130}\text{Xe}$, $^{132}\text{Xe}/^{130}\text{Xe}$ and $^{134}\text{Xe}/^{130}\text{Xe}$ ratios were then calculated by regressing against $^{136}\text{Xe}/^{130}\text{Xe}$. The ^{132}Xe -normalized fission ratios were subsequently computed and errors were propagated through each step. These compositions represent Iceland-2 and MORB-2 in Supplementary Tables 3 and 4. To investigate whether inclusion of some of the less precise measurements affect the fission deconvolution, the above analyses were re-done using a filtered data set. To use the same filtering criteria for both the MORB and Iceland data set, only data points with $^{136}\text{Xe}/^{130}\text{Xe}$ distinct from the atmospheric composition at the 2σ level and with a relative error of $<1\%$ were selected. Such filtering, however, does not affect the deconvolution significantly.

Following determination of the mantle source composition, the least-squares solution to the system $Ax = b$ was found with the following additional constraints: $\sum x_i = 1$ and $0 \leq x_i \leq 1$ (also see ref. 23). Here, A is the matrix that defines the composition of the end-members, x defines the fraction of each component, and b is the matrix with the sample composition. To compute the uncertainties, a Monte Carlo technique was used whereby the estimated sample (MORB and Iceland) compositions were varied at random within the 1σ uncertainty and the least squares fit recomputed using the new values. For all simulations, it was verified that convergence to a minimum was achieved.

In the present day mantle, $^{131,132,134,136}\text{Xe}$ isotopes reflect a mixture of the initial mantle Xe, Pu- and U-produced fission Xe, and subducted atmospheric Xe, if any. The initial Xe isotopic composition of the mantle is subject to debate. Hence, three possible initial Xe isotopic compositions were investigated: U-Xe, solar Xe, and chondritic Xe (AVCC). U-Xe and solar Xe are almost identical, except that U-Xe has a deficiency in ^{134}Xe and ^{136}Xe .

Supplementary Table 4 indicates that for all three starting mantle compositions and for both the techniques used to calculate Xe isotopic composition of the mantle source, the Iceland plume has significantly higher Pu-derived fission Xe than the MORB source. Note that for the Iceland sample, the deconvolution yields the same results within error using the two techniques (Iceland-1 and Iceland-2). For the MORB data, the deconvolution using MORB-2 gives a higher proportion of Pu-produced Xe. However, the MORB-2 composition is determined from least squares regression and, compared to the weighted mean, least squares regression may be more prone to outliers as it depends on the residual sum of squares. Nonetheless, the results in Supplementary Table 4 demonstrate that when the Iceland and MORB data sets are processed the same way, the Iceland sample, compared to MORBs, always has approximately a factor of two or higher Pu- to U-produced fission Xe. Note that for a mantle starting composition of either U-Xe, solar Xe or AVCC Xe, substantial injection of atmospheric Xe back into the mantle is required (Supplementary Table 4). The recycling of atmospheric Xe could have happened all through Earth's history associated with plate subduction or very early on in Earth's history. The requirement of subducting atmospheric Xe, however, does not change the argument that OIB Xe composition cannot be produced solely through mixing subducted Xe with MORB Xe.

The I–Pu–Xe system can constrain rates of volatile loss of a mantle reservoir through the $^{129}\text{Xe}/^{136}\text{Xe}_{\text{Pu}}$ ratio, where ^{129}Xe is the decay product of ^{129}I decay and $^{136}\text{Xe}_{\text{Pu}}$ is ^{136}Xe produced from ^{244}Pu fission. ^{129}Xe in the mantle is a mixture of initial ^{129}Xe , recycled atmospheric ^{129}Xe and radiogenic ^{129}Xe ($^{129}\text{Xe}^*$) produced from decay of ^{129}I . Once the fractions of initial ^{132}Xe and ^{132}Xe from recycled air are calculated, the $^{129}\text{Xe}/^{132}\text{Xe}$ ratio of the mantle source

(Supplementary Fig. 4) defines the fraction of ^{129}Xe produced from decay of ^{129}I ($^{129}\text{Xe}^*$). Combining this with the Pu-derived fission Xe (Supplementary Table 4) yields the $^{129}\text{Xe}^*/^{136}\text{Xe}_{\text{Pu}}$ ratio. Note that the $^{129}\text{Xe}^*/^{136}\text{Xe}_{\text{Pu}}$ ratio in the Iceland mantle is lower than in the MORB source for all three starting mantle compositions when the data sets are processed in the same way (Supplementary Table 4).